Journal of Hydrology 556 (2018) 131–142

Contents lists available at ScienceDirect

Journal of Hydrology

journal homepage: www.elsevier.com/locate/jhydrol

Research papers

Exploring the spatio-temporal interrelation between groundwater and surface water by using the self-organizing maps

I-Ting Chen [a], Li-Chiu Chang [a,*], Fi-John Chang [b,*]

[a] Department of Water Resources and Environmental Engineering, Tamkang University, New Taipei City 25137, Taiwan, ROC
[b] Department of Bioenvironmental Systems Engineering, National Taiwan University, Taipei 10617, Taiwan, ROC

ARTICLE INFO

Article history:
Received 22 December 2016
Received in revised form 7 August 2017
Accepted 9 October 2017
Available online 12 October 2017

Keywords:
Self-organizing map (SOM)
Regional groundwater
Visually display
Spatio-temporal distribution
Soft-computing method

ABSTRACT

In this study, we propose a soft-computing methodology to visibly explore the spatio-temporal groundwater variations of the Kuoping River basin in southern Taiwan. The self-organizing map (SOM) is implemented to investigate the interactive mechanism between surface water and groundwater over the river basin based on large high-dimensional data sets coupled with their occurrence times. We find that extracting the occurrence time from each 30-day moving average data set in the clustered neurons of the SOM is a crucial step to learn the spatio-temporal interaction between surface water and groundwater. We design 2-D Topological Bubble Map to summarize all the groundwater values of four aquifers in a neuron, which can visibly explore the major features of the groundwater in the vertical direction. The constructed SOM topological maps nicely display that: (1) the groundwater movement, in general, extends from the eastern area to the western, where groundwater in the eastern area can be easily recharged from precipitation in wet seasons and discharged into streams during dry seasons due to the high permeability in this area; (2) the water movements in the four aquifers of the study area are quite different, and the seasonal variations of groundwater in the second and third aquifers are larger than those of the others; and (3) the spatial distribution and seasonal variations of groundwater and surface water are comprehensively linked together over the constructed maps to present groundwater characteristics and the interrelation between groundwater and surface water. The proposed modeling methodology not only can classify the large complex high-dimensional data sets into visible topological maps to effectively facilitate the quantitative status of regional groundwater resources but can also provide useful elaboration for future groundwater management.

1. Introduction

Groundwater is a crucial resource to humans and ecosystems. In the context of sustainable water resources management, it is important to explore the mechanisms between groundwater and surface water for quantifying the amount of groundwater recharge and extraction. Modeling complex groundwater systems is one focus of current research in hydrological sciences (e.g. Bauer et al., 2006; Henriksen, et al., 2003; Wada et al., 2014). Most up-to-date researches have been directed from the development of numerical models to simulate the dynamics of surface water–groundwater interactions and/or assess the quantitative status of groundwater resources (e.g. Hartmann et al., 2015; Jan et al., 2007, Nourani and Mano, 2007; Tremblay et al., 2011). Despite great efforts put in exploring the complex spatio-temporal patterns inside groundwater data, the characteristics of aquifers remain largely unknown and modeling the dynamic complex groundwater systems is still a great challenging task with practical limitations, such as the high expense needed to overcome data availability (e.g. Anderson et al., 2015; Mohanty et al., 2015).

In watersheds with limited hydro-geophysical information, data-driven models could be a valuable alternative to extracting valuable relations inside input-output patterns and to modeling complex hydrologic systems. Artificial neural networks (ANNs) are such tools for effectively modeling nonlinear systems and capturing spatio-temporal characteristics of patterns with less computational requirements (e.g. Abrahart et al., 2012; Floreano et al., 2008; Shen and Chang, 2013). Over the last decades, ANNs have raised an increasing interest in modelling hydrological processes and therefore has led to a tremendous surge in research activities (e.g. Chang et al., 2016; Isik et al., 2013; Mekonnen et al., 2015; Mount et al., 2016; Nourani, 2017; Quiroga et al.,

* Corresponding authors.
E-mail addresses: changlc@mail.tku.edu.tw (L.-C. Chang), changfj@ntu.edu.tw (F.-J. Chang).

https://doi.org/10.1016/j.jhydrol.2017.10.015
0022-1694/

2013; Tsai et al., 2016). ANNs have also been applied with success to the temporal prediction of groundwater levels (e.g. Krishna et al., 2008, Sethi et al., 2010; Tapoglou et al., 2014; Tremblay et al., 2011; Tsai et al., 2016; Uddameri, 2007; Yoon et al., 2011). The aforementioned ANNs-based groundwater models were developed mainly to imitate single time series but rarely to model regional groundwater levels (e.g. Mohanty et al., 2015; Tsai et al., 2016). This study intends to explore the spatio-temporal dynamics of groundwater systems and assess the inter-relation of regional groundwater variations with surface water through the state-of-the-art techniques.

With very uneven rainfall, high mountains and steep-sloped rives all over the Taiwan Island constrain the storage and use of water resources. Consequently groundwater resources become vital especially during long-drought periods. In response to the industrial development and population aggregation in the last half-century, groundwater resources have been over drawn, which has caused severe subsidence and the depletion of groundwater storage space in many parts of the island (Chen, et al., 2007; Hung, et al., 2012; Wada, et al., 2012). Effective groundwater resources management is a crucial task. The subsidence and large variations of groundwater levels over the decades suggest a precise and detailed study is required for elucidating the behavior of groundwater fluctuations in both spatial and temporal scales. The purpose of this study was thus to comprehensively investigate and model regional groundwater variations for sustainable management of groundwater resources. The variation of groundwater in the whole basin was analyzed by using a clustering method to identify the spatio-temporal characteristics of groundwater levels. We proposed a soft-computing technique that can visibly describe and foresee the complex-dynamic regional groundwater variations at high spatial and temporal resolutions.

The paper is organized into five sections. The first section introduces the general background and ideas used in this study. The second section describes the study area and datasets used in modeling processes. The third section describes the methodology and focuses on how the ANN models can be implemented to model regional groundwater levels. The fourth section presents the results of scenario calculations relevant to regional water resources management. The final section summarizes the results and gives conclusions regarding the coupled surface water/groundwater systems in semiarid regions.

2. Study area and dataset

The Kuoping River basin is the largest drainage basin (3257 km^2) in Taiwan, and the river meanders 171 km through a highly rugged terrain in the Central Mountain Range towards the southern part of Taiwan Strait, where the Pingtung Plain is situated with rich groundwater resources (Fig. 1). The mean annual rainfall of this basin is close to 3000 mm, while over 90% of which appears in the wet season during May and October, which is influenced by typhoons and monsoons. The amount of the wet-season flow would increase approximately 10 times than that of the dry-season flow. The extremely uneven distribution of rainfall and stream flows over seasons has resulted in a severe issue of water resources management. The basin is primarily planned for agricultural productions and stock farms, while the latest development of fish farms and industrial complexes requires more water. Due to the tremendous water demands that continue growing inevitably, the over-exploitation of groundwater by different sectors has caused a severe drop of groundwater levels and subsidence and thus has imposed great pressure on the environment.

To better learn the status and effectively manage the vital groundwater resources in the study basin, we collected the basin-wide daily hydrological monitoring data sets (during 1999 and 2015) to perform the data-mining analysis and model construction. 126 time series of groundwater levels and three time series of river flow were obtained from the Water Resources Agency (WRA), Taiwan. Thirteen time series of precipitation were obtained from the Central Weather Bureau, Taiwan. Fig. 1 shows the locations of the study area and monitoring stations, and Fig. 2 shows the geological characteristics of the basin, where four thick aquifers can be found in various areas.

3. Methodology

In this study, we explore the spatio-temporal dynamics of groundwater systems through the soft-computing techniques that can visibly describe and foresee the complex-dynamic regional groundwater variations. The large high-dimensional data sets coupled with their occurrence times are analyzed, and the proposed methodology is presented as follows.

3.1. Data preprocessing

In order to eliminate the elevation effects of different observational groundwater wells, we adopted the relative groundwater level (RGL), i.e. the groundwater water level was subtracted by the minimum value of historical observed groundwater levels, as shown in Eq. (1), in this study.

$$WL_{i,\mathrm{Relative}} = WL_{i,\mathrm{Original}} - WL'_{i,\min} \quad (1)$$

where i represents the ith well, $WL_{i,\mathrm{Relative}}$ represents the relative groundwater level, $WL_{i,\mathrm{Original}}$ represents the original groundwater level, and $WL'_{i,\min}$ represents the minimum value of the original (historical) groundwater levels.

The moving average method is commonly used with time series data to smooth out short-term fluctuations and highlight longer-term trends and/or cycles, and the produced data sets are logically coherent in the time domain. We used 30-day moving average to analyze data points by creating a series of data, each of which was averaged over a subset (30 daily data) of the original RGL data set (ranging between 1999/01/01 and 2015/12/2). The 30-day moving average of RGLs was calculated, where a total of 6180 data sets were obtained and each data set included the RGLs of 126 wells. Table 1 summarizes the groundwater, precipitation and flow records in the last sixteen years (1999–2015) used in this study.

3.2. SOM overview

The self-organizing map (SOM) proposed by Kohonen (1982) is a powerful method used to explore the interrelationships of high-dimensional multivariate systems, and it is effective for clustering and forecasting in a wide-spread range of disciplines. A key benefit of the SOM is its ability to extract implicit patterns from high-dimensional input data sets and classify the obtained patterns into a low-dimensional output layer, where similar inputs remain close together in the output neurons while preserving data structure. The neurons in the output layer are commonly arranged in two-dimensional grids so that the constructed topology can be visualized to give an insight into the system under investigation. The SOM has gained increasing interest and been successfully applied to water resources management. A number of promising researches related to the modeling of groundwater processes are briefly reviewed as follows. For instance, Hassan et al. (2014) modeled the structural and hydrological complexity of hard rock systems affecting the dynamics of surface–groundwater

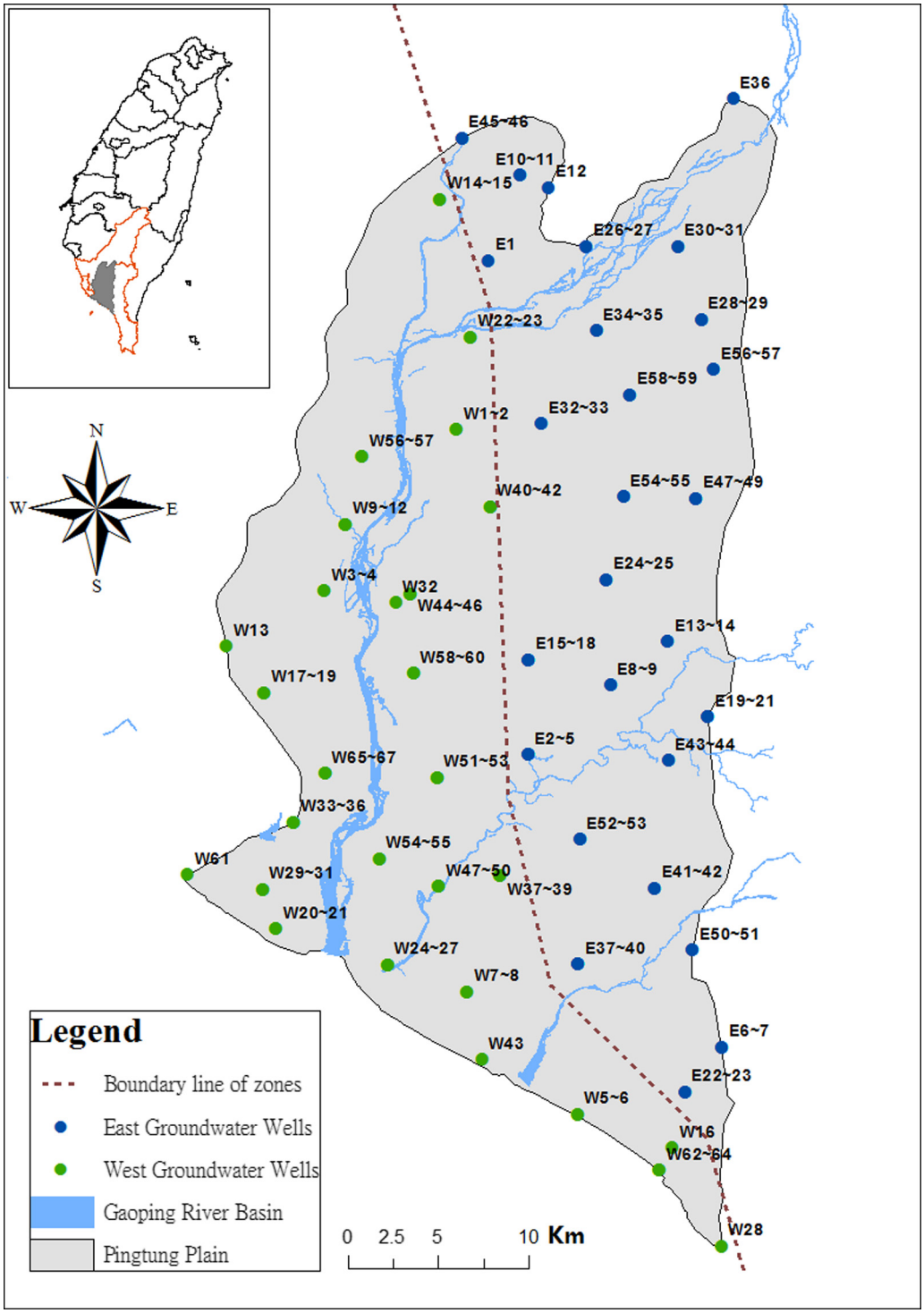

Fig. 1. Locations of groundwater wells installed with 126 sensors spreading over four aquifers in the Pingtung Plain of Taiwan.

interactions; Krause et al. (2007) indicated that the interactions of the investigative system could be characterized by temporal and spatial variability; Tremblay et al. (2011) found drastically different patterns of variability evolution for the records in three Canadian regions; and Jan et al. (2007) indicated the effective accumulated rainfall amount highly-correlated to the difference between groundwater levels at each moment. Recently, the SOM has been satisfactorily applied to regionalization studies (e.g. Agarwal, et al., 2016; Chang et al., 2016) and watershed classification (e.g. Ley et al., 2011; Razavi and Coulibaly, 2017).

3.3. Configure the SOM

This study configured an SOM to cluster a large number of high-dimensional regional RGLs into a visible 2-dimensional topology of regional RGL maps. The map size of the SOM must be determined at first. Even though we did have a large number of data sets, which, however, were logically coherent in the time domain due to the 30-day moving average procedure conducted to synthesize the time series data sets. Consequently, we only tried a few map sizes (i.e. $3 * 3$, $4 * 4$ and $5 * 5$). The constructed

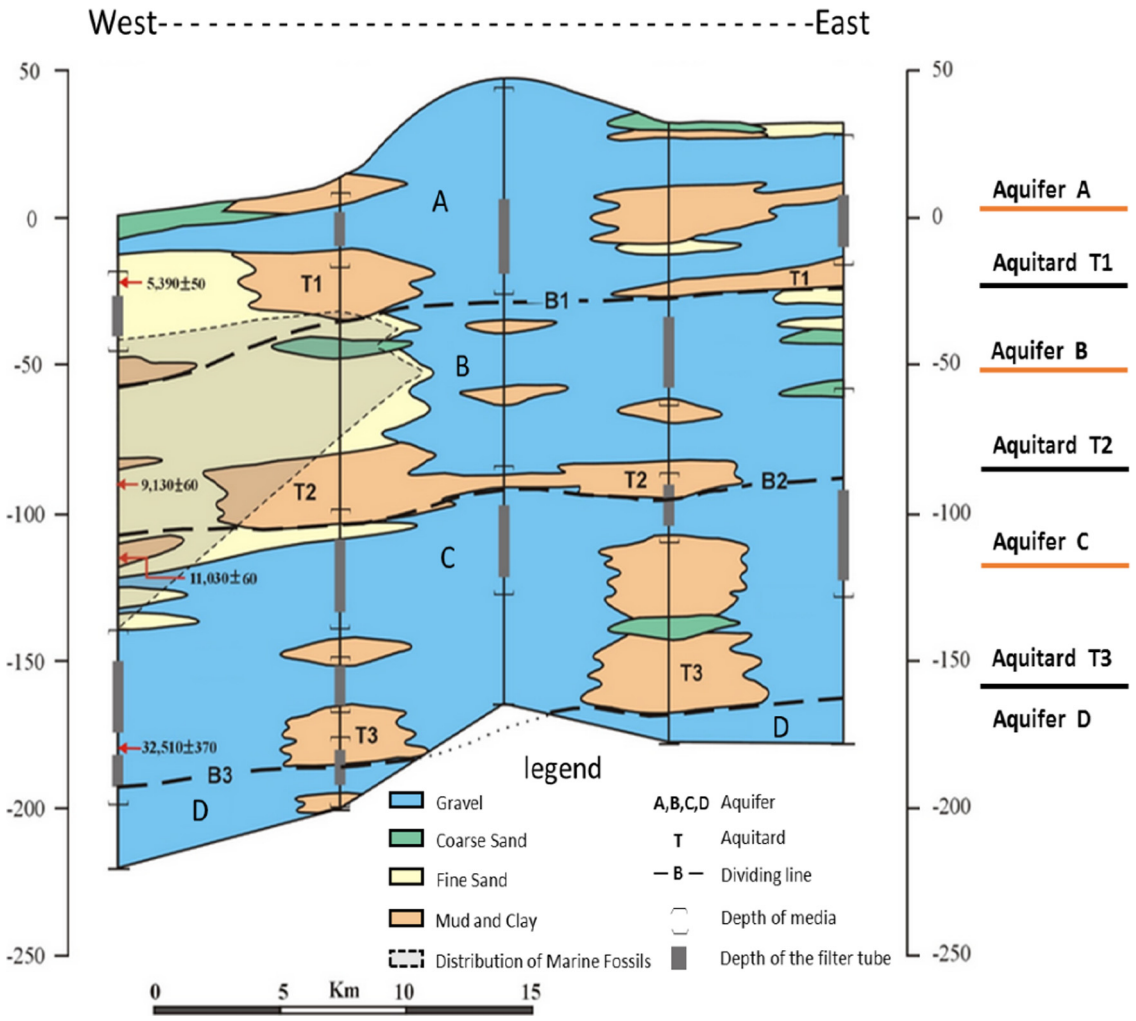

Fig. 2. Geological setting of the main stratigraphic compositions in the Pingtung Plain (modified from the original map provided by the Central Geological Survey, MOEA, Taiwan).

Table 1
Basic statistics of relative groundwater levels, rainfall and river flow in the last sixteen years (1999–2015).

Aquifers	Number of stations	
	East	West
A	18	21
B	20	13
C	14	19
D	7	14
Total	E1–E59	W1–W67

Month	RGL (m)		Rainfall (mm)	Flow (cm)
	East	West		
1	6.03	3.01	19	72
2	4.76	2.72	24	68
3	3.61	2.44	35	72
4	2.66	2.18	90	80
5	2.33	2.15	360	184
6	4.73	2.72	578	453
7	7.15	3.17	663	477
8	9.27	3.82	766	631
9	10.31	4.15	444	455
10	9.86	3.99	123	222
11	8.53	3.69	44	116
12	7.30	3.45	38	84
Mean	6.38	3.12		

topological maps coupled with related key features (Averaged RGL and weights) of aquifer B were shown in Fig. 3. The results indicated that (1) the small network (i.e. 3 * 3) could not fully present the regional RGL classification, while there were many similar clusters in the large network (5 * 5), and (2) the 4 * 4 network was considered the most suitable for presenting the topology of regional RGL classification. The 126 RGLs were distributed in four heterogeneous aquifers, and the groundwater monitoring wells were discontinuous with respect to vertical aquifers. The three dimensional problem could not be well presented in a 2-dimensional SOM map. Consequently, we made a 2-dimensional SOM map for each aquifer. To better display the variation of RGLs

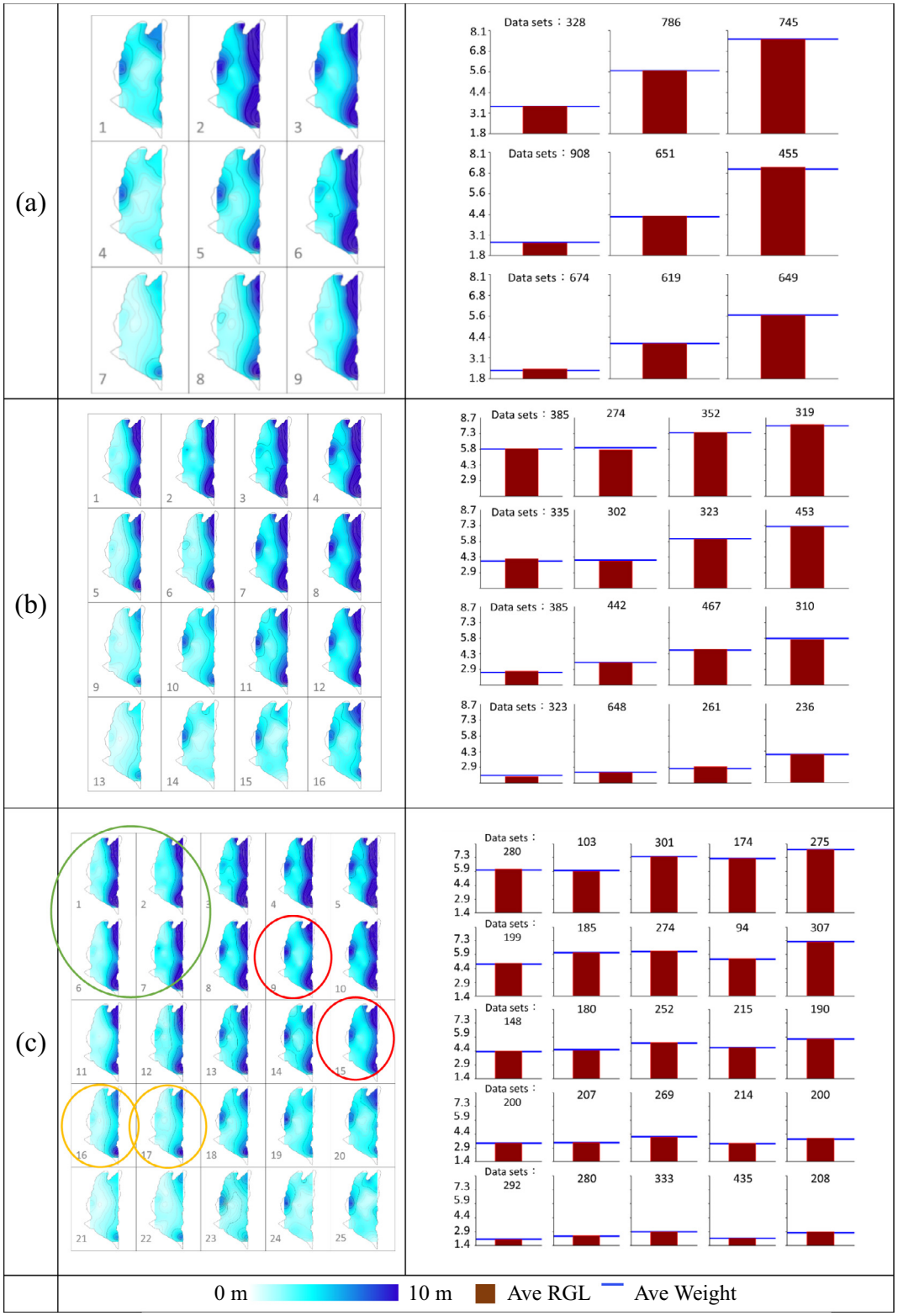

Fig. 3. The constructed (a) 3 * 3, (b) 4 * 4, and (5 * 5) SOM topological maps coupled with their key features of aquifer B.

in each aquifer, the Ordinary Kriging method was used to connect RGLs within an aquifer to form a 2-dimensional SOM map for presenting the spatial distribution of RGLs in the aquifer. The Kriging is an interpolation method that gives the best unbiased linear estimation of the intermediate values and is widely used in the domain of spatial analysis (e.g. Tapoglou, et al., 2014, Parajka, et al., 2015; Piazza, et al., 2015).

We intended to classify and quantify the large complex high-dimensional data sets based on soft-computing techniques (SOM topological maps) and make a comprehensive analysis of groundwater variations in four aquifers to learn and present their spatio-temporal features. The comprehensive analytical framework is shown in Fig. 4, which can be divided into four major schemes presented as follows.

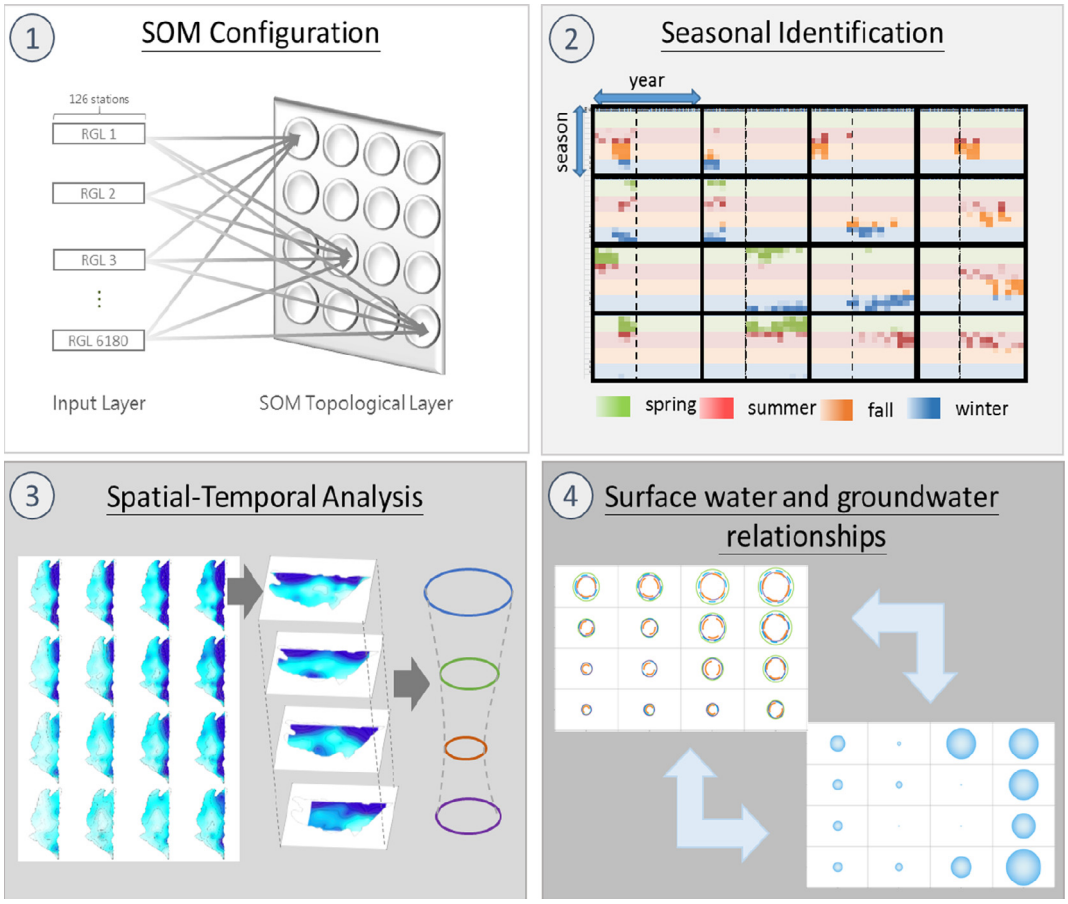

Fig. 4. Research flow chart of the study.

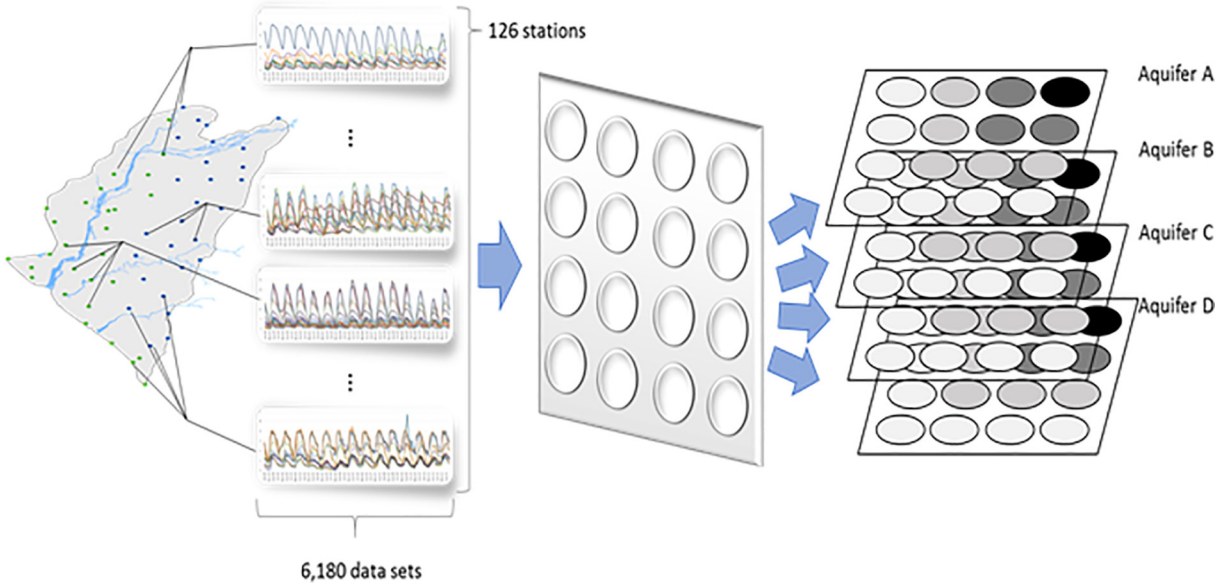

Fig. 5. Relative groundwater levels classified by the SOM (4x4 neurons).

Scheme 1: SOM configuration

A 4 * 4 SOM network was configured based on large data sets (i.e. 6180), where each data included 126 RGLs (Fig. 5). Because the wells were distributed in four aquifers, the configured SOM would be thus displayed in four topological maps for the corresponding aquifers, respectively.

Scheme 2: Seasonal identification

As the SOM was configured, we could identify the temporal information of the clustered data sets in each neuron in a seasonal scale for allocating these data into four seasons.

Scheme 3: Spatio-temporal analysis

The RGL topological maps in four aquifers could be obtained. The Kriging method was applied to drawing the RGL distribution of the neurons. Thus, the RGLs of four aquifers could thus be fully visualized. To easily tell the differences and interrelation, we designed a "2-D Topological Bubble Map" to merge all the averaged RGL values of four aquifers in a neuron so that the vertical relations could be quantified into the "Topological Bubble Map". The whole multi-dimensional data sets could then be summarized and therefore we could visibly explore the major features of the RGLs in the vertical direction.

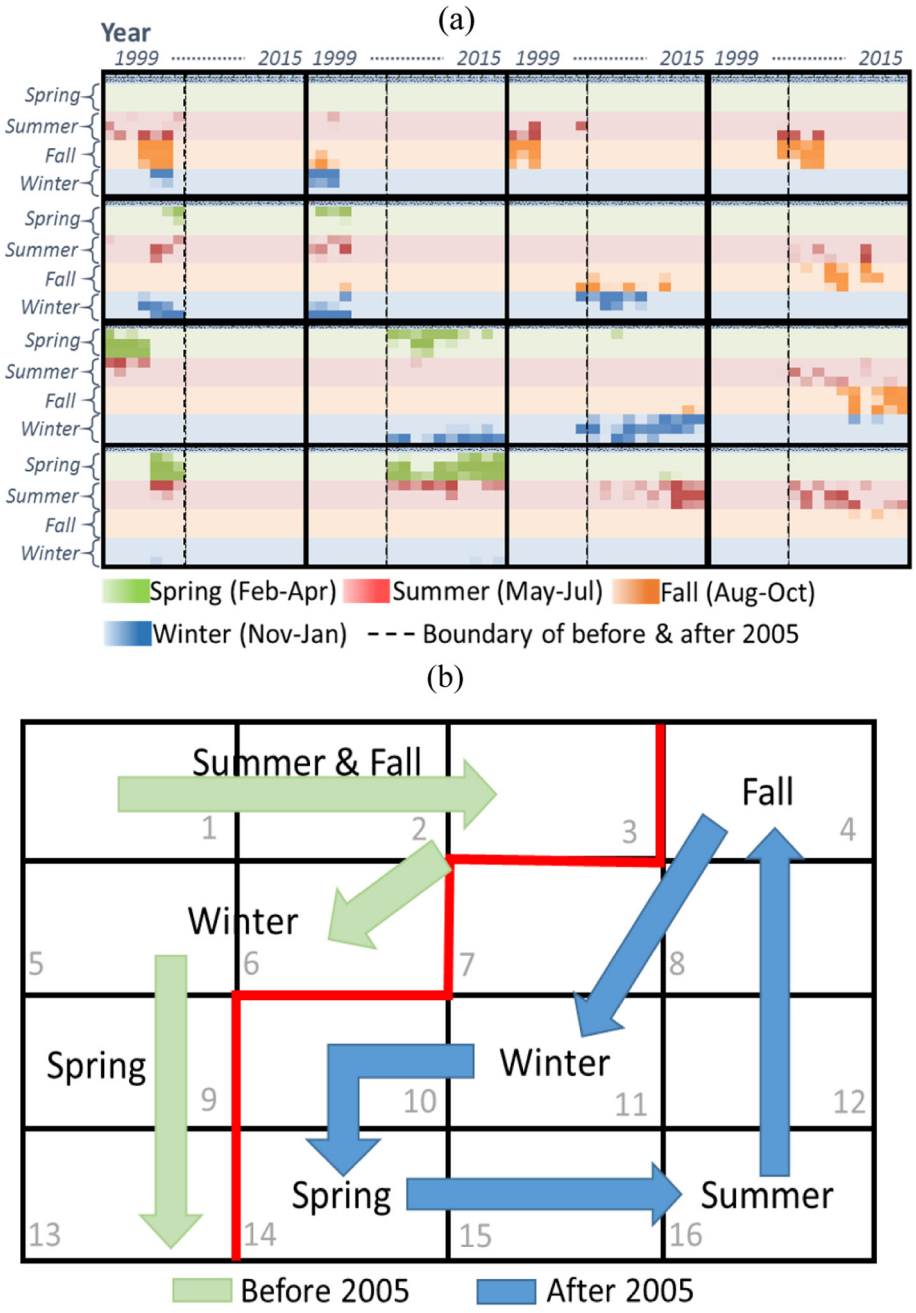

Fig. 6. Temporal distribution displayed in each neuron, which prominently shows seasonal changes between neurons. (For interpretation of the references to colour in this figure legend, the reader is referred to the web version of this article.)

Scheme 4: Surface water and groundwater relationships

To assess the possible relations between surface water and groundwater, we computed the average rainfall and flow amounts in a neuron, which represented the surface water information in a specific time interval of the corresponding neuron, and put all the information (surface water and RGLs in four aquifers) together so that we could easily examine the possible relationship inside the topological features maps.

4. Results and discussion

As mentioned above, the 30-day moving average procedure was used to synthesize the analyzed data, and a total of 6180 data sets, where each data set included 126 RGLs, were obtained and used for constructing the SOM. To excavate the temporal-spatial features inside the SOM, the time and average RGL in each neuron were analyzed. We discovered a topological feature shift before & after 2005 through the decomposition of the SOM data structure, and the similarities of datasets could be organized by year and by season. Fig. 6(a) indicates the occurrence time of the clustered data sets in each neuron (years 1999–2015; season coloring: spring_green, summer_red, fall_pink, winter_blue; the darker color meant more data sets were included in a dot), and Fig. 6(b) shows the seasonal changes (moves) between neurons. We noticed that the data collected before & after 2005 could be easily separated (the dotted line in each neuron in Fig. 6(a) & the red line in (b)), and such phenomenon might be due to the "Regulations on Groundwater Conservation" implemented by the Government in 2002 and a great number of farm's pumping well were shut down in the following years. The seasonality of each neuron could also be easily identified because the occurrence times of the data in each group fell within the same season (Fig. 6(b)). As we assessed in more details, we found that the neurons well presented a seasonal loop, i.e. neurons before 2005 formed another cycle, where the seasonal direction of the group again started from summer to fall (#1, # 2, #3), then moved to winter (#5, #6), and finally ended in spring (#9, #13). Neurons after 2005 formed a cycle, where the seasonal direction of the group started from summer toward fall (#16, #12, #8, #4), then moved to winter (#7, #11), and eventually returned to summer (#15, #16) by passing through spring (#14). The seasonal cycles in the map indicated the neighborhood features of the topology and provided extra evidence of the sustained persistent phenomenon in groundwater levels. We also calculated the average value of the RGLs in each neuron of the constructed SOM for each aquifer, and the clustering statistics, including the number of data, rainfall, stream flow, and the average RGL, in each neuron of the SOM are summarized in Table 2.

The regional RGL distribution was drawn by the Kriging spatial interpolation method. Fig. 7 displays the horizontal topological classification of the regional RGLs in four aquifers (A–D). They could be visualized and explored, where the RGL value increased from the lower left corner (neuron #13) to the upper right corner (neuron #4) in the topological distribution. It clearly indicated that the groundwater level gradually decreased from east to west over the entire area, which re-confirms the permeability of the eastern area is much greater than that of the western area (Fig. 2). It was easy to tell the spatial variation in the neurons, where the RGL gradually increased from west to east over the entire area (i.e. light color in the western area and dark color in the eastern area).

Table 2
The RGL value of each neuron in different aquifers (A, B, C, D) extracted from SOM model.

Neuron	1	2	3	4
Number	460	230	333	367
R*	297	84	561	559
F*	299	132	688	618
A	5.40	5.29	6.96	7.46
B	7.35	7.34	9.20	9.92
C	6.32	6.81	7.93	8.57
D	5.61	6.14	6.97	7.67
Neuron	5	6	7	8
Number	315	357	359	312
R	194	134	32	561
F	262	105	125	398
A	3.63	3.77	5.62	6.77
B	4.86	5.09	7.78	8.91
C	4.51	4.92	7.08	7.71
D	4.23	4.68	6.60	7.15
Neuron	9	10	11	12
Number	376	528	501	434
R	178	36	29	457
F	116	84	91	370
A	2.49	3.28	4.33	5.37
B	3.22	4.36	5.97	7.01
C	3.30	4.24	5.52	6.00
D	3.30	4.40	5.40	5.68
Neuron	13	14	15	16
Number	300	766	290	252
R	179	155	396	659
F	135	120	238	409
A	2.14	2.26	2.80	3.88
B	2.69	2.83	3.37	5.00
C	2.79	2.90	3.13	4.29
D	2.94	3.24	3.53	4.53

* R and F denote precipitation (mm) and flow (cms), respectively.

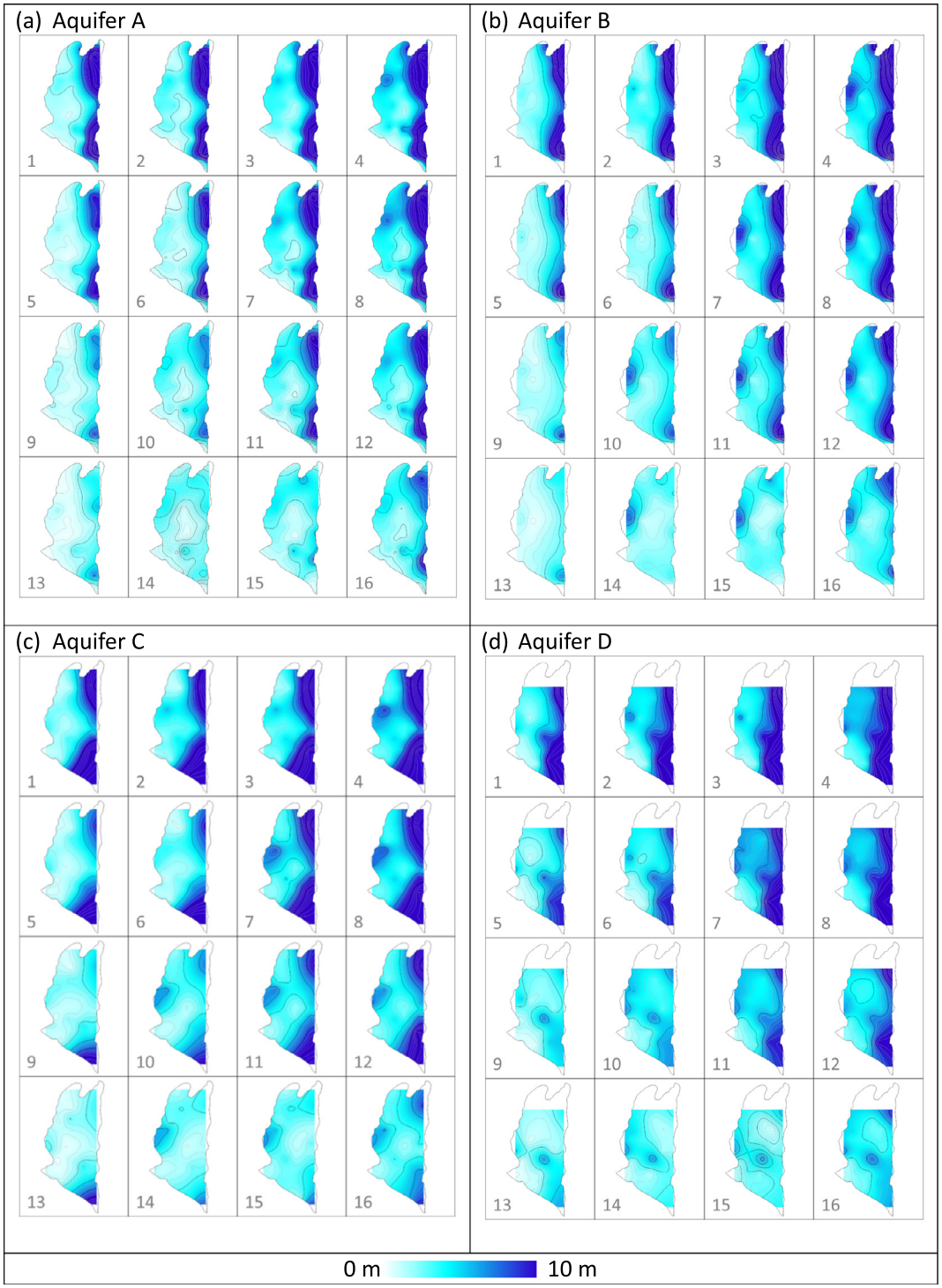

Fig. 7. The SOM topological maps of aquifers A, B, C and D in the Pingtung Plain. The RGLs of each aquifers were classified into 16 groups (neurons) and showed the neighboring relationship of water level changes.

As we integrated Fig. 6 with Fig. 7, we could catch the regional groundwater variation maps of all the four aquifers in different periods of time (season).

We designed a 2-D Topological Bubble Map to integrate all the information in the same neuron (cluster) together to elaborate the link between climate, surface waters, and groundwater in four aquifers. The inter-relational features of groundwater variations in four aquifers with rainfall and streamflow could be visibly found from the designed "2-D topological bubble map", where the groundwater variations in the four aquifers were presented by 4 circles (Fig. 8(a)) and the amounts of rainfall and streamflow were presented by one circle (Fig. 8(b) and (c)), respectively, for each clustered neuron. A larger circle means a larger value of the corresponding variable.

Fig. 8(a) shows the general features and trends of groundwater variations in different seasons as well as in various aquifers (vertical analysis). The higher the RGL is, the bigger the circle (bubble) is. Aquifer B has the biggest bubble indicated that Aquifer B received

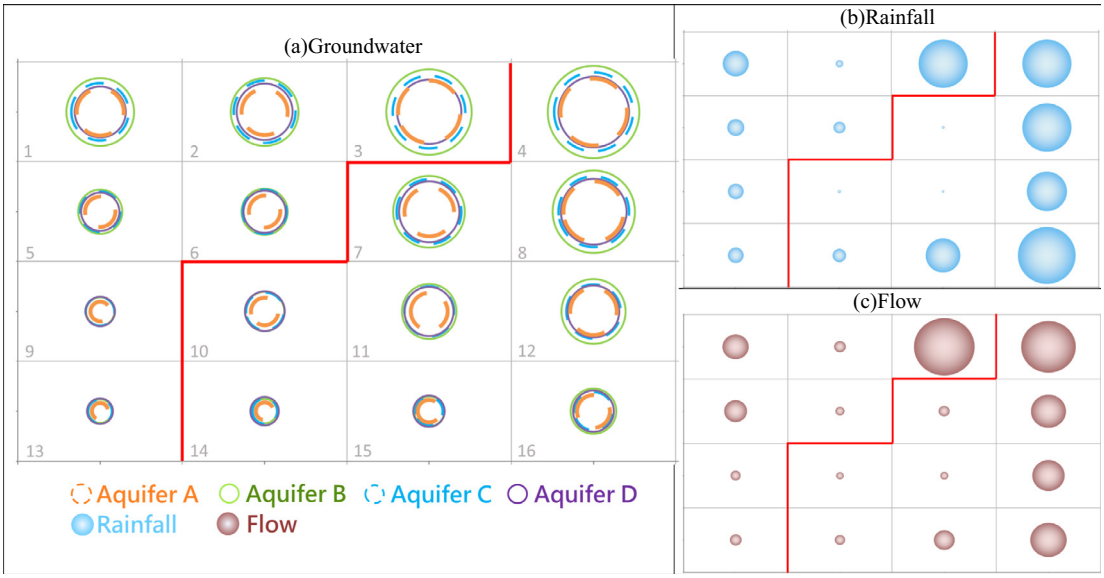

Fig. 8. Topological maps of surface water and groundwater in four aquifers. A larger circle represents a higher value.

more recharge quantity than the other aquifers and tended to be more easily refilled. As we investigated the distribution of the temporal topology after 2005 (Fig. 6(a)), the water level was gradually brimmed to the top from summer to fall (neurons #16, #12, #8, #4). When winter came, the water level slightly reduced (neurons #4, #7, #11). The minimum water level occurred between winter and spring (neurons #11, #10, #14). A sharp drawdown could be observed from the outer ring to the inner ring in Aquifer B. The water level in Aquifer A dropped to the lowest value. The water level gradually increased again until summer returned (neurons #14, #15, #16), wherein the inner ring was displaced by the outer ring in Aquifer B.

The results indicated that rainfall and flow was highly correlated and higher rainfall (as well as flow) occurred in summer and fall, as presented in neurons #4, #8, #12 and #16. Besides, rainfall significantly decreased from fall to winter. The groundwater levels in all layers only slightly reduced in fall, which might be due to the recharge from upstream (mountain area) groundwater outflow and/or river flow for replenishing underground aquifers. The groundwater level in winter (neurons #7, #11, #10) still maintained in an average level even though there was no much rainfall in this season. We also noticed that river flow still occurred in winter which might mainly come from groundwater outflow. Even though rainfall would slightly increase as spring arrived, the groundwater level fell from winter to the next spring and the water level in spring reached the lowest groundwater level (minimum circle) in a year.

Based on the pattern analysis on the visualizing SOM maps, the inter-relationships of groundwater among various aquifers can be identified and the interactions between groundwater and surface water can also be sketched. Uncertainty due to obscured spatial characteristics of regional groundwater is a long-standing challenge issue for effective groundwater management. The SOM approach presented here utilizes the pattern classification capability of a neural network and its ability to learn from a large number of data sets. The constructed feature maps not only can meaningfully present the spatio-temporal characteristics of regional groundwater but also display its interaction with surface water. This joint approach enables one to visibly quantify their uncertainty inside the SOM, which provide regional features and useful information for sustainable management of groundwater resources. There is, however, a large variability in groundwater residence time, including groundwater flow paths that discharge groundwater into surface water. Consequently, it is still difficult to quantify the groundwater recharge amount refilling aquifer storage and the groundwater discharge amount releasing back to surface water and becoming runoff based on the limited clusters (ex. 16 clusters obtained in this study). A more sophisticate modeling technique with long-term comprehensive monitoring data sets, such as daily (even hourly) data including regional groundwater and rainfall data and a series of flow data along the river from upstream to downstream, and hydrogeological features in the study area might be necessary to precisely identify and/or estimate the discharge and recharge amounts of groundwater.

As mentioned early, modeling complex groundwater systems to simulate the dynamics of surface water–groundwater interactions and/or assess the quantitative status of groundwater resources is still a great challenging task. In this study, we implemented the data-driven techniques for configuring the SOM feature map through decomposing the large high-dimensional 30-day moving average RGL data sets that could help to better understand how the spatio-temporal characteristics of 126 groundwater sensors and the multi-relations among hydrological variables. We designed a number of figures to display and explore the complex dynamic temporal-spatial groundwater and surface water characteristics, where Fig. 6 displayed the temporal distribution of each neuron and seasonal changes between neurons, Fig. 7 shown the clustered RGL topological maps of four aquifers in the Pingtung Plain, and Fig. 8 presented the 2-D bubble topological maps of surface water and RGL in four aquifers, which integrated all the information in all the clustered neuron to explore their complex dynamic temporal-spatial characteristics and discover the regional groundwater variations in various aquifers.

5. Conclusions

In this study, we conducted a study to explore the complex spatial-temporal groundwater features and multi-relations among hydrological variables in the Kuoping river basin based on a systematic combination of large (i.e. 6180) data sets of high-dimensional groundwater levels (126 RGLs) in various aquifers, rainfall and stream flow by using the data-driven techniques. Distinct patterns of regional groundwater characteristics and specific

dominant hydrological attributes could be identified in the clusters obtained from the nonlinear clustering techniques, the SOM, which indicated the obtained clustering results were sound from the hydrological point of view. The major findings based on the constructed topological maps of the SOM in the four aquifers of the study area are summarized as follows.

1. Extracting the occurrence time of each 30-day moving average data set in the clustered neurons of the SOM is a crucial step to identify the spatio-temporal interaction between surface water and groundwater.
2. The constructed topological maps clearly indicate that the fluctuation of groundwater level decreases from east to west in the Pingtung Plain, which re-confirms the permeability of the eastern area is much greater than that of the western area.
3. The water levels in four aquifers have different growth and decline patterns in various seasons. The water level fluctuations in Aquifers B and C are more significant than those of the other two layers, which indicate those two layers can be more easily replenished or drained out.
4. The regional water levels possess a seasonal cycle before and after the 2005, respectively. They gradually increase from spring to summer, dramatically increase to reach the maximum in fall, then gradually decease from fall to the next spring, and consequently reached the minimum in spring.
5. The designed "2-D Topological Bubble Map", which summarizes all the averaged RGL values of four aquifers and surface water in a neuron, can visualize the major features of the RGLs in the vertical direction, so that we could easily examine the interrelationships of groundwater among various aquifers and the interactions between groundwater and surface water.

In sum, we classified the complex high-dimensional data sets based on the topological maps to make a comprehensive analysis of groundwater variations in four aquifers and present their spatio-temporal features. The SOM results could visibly explore the behavior of regional groundwater variations in various aquifers, present the seasonal cycles in a temporal scale, and systematically classify the interactions between surface water and groundwater, and obtain the spatio-temporal interrelation. We thus conclude that the constructed feature maps are topologically ordered in the sense that the spatial location of a neuron in the lattice corresponds to the particular features of input patterns and can meaningfully present the spatio-temporal characteristics of regional groundwater and its interaction with surface water, which provide useful elaboration for future groundwater management plans.

Acknowledgments

This study was supported by the Water Resources Agency, Taiwan, ROC. (Grant number: MOEAWRA1040062). Streamflow and groundwater level data were provided by the Water Resources Agency, rainfall data were provided by the Central Weather Bureau, and the geological map was provided by the Central Geological Survey, Taiwan, ROC. We feel gratitude to Editors and Reviewers for providing valuable comments and constructive suggestions.

References

Abrahart, R.J., Anctil, F., Coulibaly, P., Dawson, C.W., Mount, N.J., See, L.M., Shamseldin, A.Y., Solomatine, D.P., Toth, E., Wilby, R.L., 2012. Two decades of anarchy? Emerging themes and outstanding challenges for neural network river forecasting. Prog. Phys. Geogr. 36 (4), 480–513.

Agarwal, A., Maheswaran, R., Kurths, J., Khosa, R., 2016. Wavelet Spectrum and self-organizing maps-based approach for hydrologic regionalization – a case study in the western United States. Water Resour. Manage. 30 (12), 4399–4413.

Anderson, M.P., Woessner, W.W., Hunt, R.J., 2015. Applied Groundwater Modeling: Simulation of Flow and Advective Transport. Academic Press.

Bauer, P., Gumbricht, T., Kinzelbach, W., 2006. A regional coupled surface water/groundwater model of the Okavango Delta, Botswana. Water Resour. Res. 42 (4). https://doi.org/10.1029/2005WR004234.

Chang, F.J., Chang, L.C., Huang, C.W., Kao, I.F., 2016. Prediction of monthly regional groundwater levels through hybrid soft-computing techniques. J. Hydrol. 541, 965–976.

Chen, C.T., Hu, J.C., Lu, C.Y., Lee, J.C., Chan, Y.C., 2007. Thirty-year land elevation change from subsidence to uplift following the termination of groundwater pumping and its geological implications in the Metropolitan Taipei Basin, Northern Taiwan. Eng. Geol. 95 (1), 30–47.

Floreano, D., Dürr, P., Mattiussi, C., 2008. Neuroevolution: from architectures to learning. Evol. Intel. 1 (1), 47–62.

Hartmann, A., Gleeson, T., Rosolem, R., Pianosi, F., Wada, Y., Wagener, T., 2015. A large-scale simulation model to assess karstic groundwater recharge over Europe and the Mediterranean. Geosci. Model Dev. 8, 1729–1746.

Hassan, S.M.T., Lubczynski, M.W., Niswonger, R.G., Su, Z., 2014. Surface–groundwater interactions in hard rocks in Sardon catchment of western Spain: an integrated modeling approach. J. Hydrol. 517, 390–410.

Henriksen, H.J., Troldborg, L., Nyegaard, P., Sonnenborg, T.O., Refsgaard, J.C., Madsen, B., 2003. Methodology for construction, calibration and validation of a national hydrological model for Denmark. J. Hydrol. 280, 52–71.

Hung, W.C., Hwang, C., Liou, J.C., Lin, Y.S., Yang, H.L., 2012. Modeling aquifer-system compaction and predicting land subsidence in central Taiwan. Eng. Geol. 147–148, 78–90.

Isik, S., Kalin, L., Schoonover, J.E., Srivastava, P., Lockaby, B.G., 2013. Modeling effects of changing land use/cover on daily streamflow: an artificial neural network and curve number based hybrid approach. J. Hydrol. 485, 103–112.

Jan, C.D., Chen, T.H., Lo, W.C., 2007. Effect of rainfall intensity and distribution on groundwater level fluctuations. J. Hydrol. 332 (3), 348–360.

Kohonen, T., 1982. Self-organized formation of topologically correct feature maps. Biol. Cybern. 43, 59–69.

Krause, S., Bronstert, A., Zehe, E., 2007. Groundwater–surface water interactions in North German lowland floodplain–implications for the river discharge dynamics and riparian water balance. J. Hydrol. 347 (3), 404–417.

Krishna, B., Satyaji Rao, Y.R., Vijaya, T., 2008. Modelling groundwater levels in an urban coastal aquifer using artificial neural networks. Hydrol. Process. 22 (8), 1180–1188.

Ley, R., Casper, M.C., Hellebrand, H., Merz, R., 2011. Catchment classification by runoff behaviour with self-organizing maps (SOM). Hydrol. Earth Syst. Sci. 15 (9), 2947–2962.

Mekonnen, B.A., Nazemi, A., Mazurek, K.A., Elshorbagy, A., Putz, G., 2015. Hybrid modelling approach to prairie hydrology: fusing data-driven and process-based hydrological models. Hydrol. Sci. J. 60 (9), 1473–1489.

Mohanty, S., Jha, M.K., Raul, S.K., Panda, R.K., Sudheer, K.P., 2015. Using artificial neural network approach for simultaneous forecasting of weekly groundwater levels at multiple sites. Water Resour. Manage. 29 (15), 5521–5532.

Mount, N.J., Maier, H.R., Toth, E., Elshorbagy, A., Solomatine, D., Chang, F.J., Abrahart, R.J., 2016. Data-driven modelling approaches for socio-hydrology: opportunities and challenges within the Panta Rhei Science Plan. Hydrol. Sci. J. 61 (7), 1192–1208.

Nourani, V., 2017. An emotional ANN (EANN) approach to modeling rainfall-runoff process. J. Hydrol. 544, 267–277.

Nourani, V., Mano, A., 2007. Semi-distributed flood runoff model at the subcontinental scale for southwestern Iran. Hydrol. Process. 21 (23), 3173–3180.

Parajka, J., Merz, R., Skøien, J.O., Viglione, A., 2015. The role of station density for predicting daily runoff by top-kriging interpolation in Austria. J. Hydrol. Hydromech. 63 (3), 228–234.

Piazza, A.D., Conti, F.L., Viola, F., Eccel, E., Noto, L.V., 2015. Comparative analysis of spatial interpolation methods in the Mediterranean area: application to temperature in Sicily. Water 7 (5), 1866–1888.

Quiroga, V.M., Popescu, I., Solomatine, D.P., Bociort, L., 2013. Cloud and cluster computing in uncertainty analysis of integrated flood models. J. Hydroinform. 15 (1), 55–70.

Razavi, T., Coulibaly, P., 2017. An evaluation of regionalization and watershed classification schemes for continuous daily streamflow prediction in ungauged watersheds. Can. Water Resour. J./Revue canadienne des ressources hydriques 42, 2–20.

Sethi, R.R., Kumar, A., Sharma, S.P., Verma, H.C., 2010. Prediction of water table depth in a hard rock basin by using artificial neural network. Int. J. Water Resour. Environ. Eng. 2 (4), 95–102.

Shen, H.Y., Chang, L.C., 2013. Online multistep-ahead inundation depth forecasts by recurrent NARX networks. Hydrol. Earth Syst. Sci. 17 (3), 935–945.

Tapoglou, E., Karatzas, G.P., Trichakis, I.C., Varouchakis, E.A., 2014. A spatio-temporal hybrid neural network-Kriging model for groundwater level simulation. J. Hydrol. 519, 3193–3203.

Tremblay, L., Larocque, M., Anctil, F., Rivard, C., 2011. Teleconnections and interannual variability in Canadian groundwater levels. J. Hydrol. 410 (3), 178–188.

Tsai, W.P., Chiang, Y.M., Huang, J.L., Chang, F.J., 2016. Exploring the mechanism of surface and ground water through data-driven techniques with sensitivity analysis for water resources management. Water Resour. Manage. 30 (13), 4789–4806.

Uddameri, V., 2007. Using statistical and artificial neural network models to forecast potentiometric levels at a deep well in South Texas. Environ. Geol. 51 (6), 885–895.

Wada, Y., van Beek, L.P.H., Weiland, F.C.S., Chao, B.F., Wu, Y.H., Bierkens, M.F.P., 2012. Past and future contribution of global groundwater depletion to sea-level rise. Geophys. Res. Lett. 39, L09402. https://doi.org/10.1029/2012GL051230.

Wada, Y., Wisser, D., Bierkens, M.F.P., 2014. Global modeling of withdrawal, allocation and consumptive use of surface water and groundwater resources. Earth Syst. Dyn. 5 (1), 15–40.

Yoon, H., Jun, S.C., Hyun, Y., Bae, G.O., Lee, K.K., 2011. A comparative study of artificial neural networks and support vector machines for predicting groundwater levels in a coastal aquifer. J. Hydrol. 396, 128–138.